Journal of Non-Crystalline Solids 358 (2012) 3318–3321

Contents lists available at SciVerse ScienceDirect

Journal of Non-Crystalline Solids

journal homepage: www.elsevier.com/locate/jnoncrysol

Hardness and free volume distributions of Zr-based alloys spot treated by laser beam

W. Zhao, G. Li *, Y.Y. Wang, R.P. Liu

State Key Laboratory of Metastable Materials Science and Technology, Yanshan University, Qinhuangdao 066004, P. R. China

ARTICLE INFO

Article history:
Received 4 June 2012
Received in revised form 13 August 2012
Available online 4 October 2012

Keywords:
Free volume;
Laser treatment;
Metallic glass;
Finite element analysis

ABSTRACT

A fixed laser beam heat source was used to re-melt Zr-based crystalline and amorphous alloys. Four hardness regions are found in the amorphous sample along the radial direction of the spot treated by laser beam, whereas two hardness regions are found in the crystalline sample. Results indicate that the hardness of the crystalline phase is lower than that of the amorphous phase. The hardness of the amorphous phase increases with reducing free volume and nanoholes.

1. Introduction

In the early 1990s, Zr-based amorphous alloy systems were found to have the largest glass-forming ability in the alloy body department. Zr-based amorphous alloys do not contain noble metals and have excellent mechanical, physical, and chemical properties. However, poor plasticity in normal conditions makes Zr-based amorphous alloys prone to brittle fracture. By contrast, Zr-based crystalline alloys have good plasticity but relatively low hardness and poor resistance to abrasion. Thus, decrystallization of Zr-based crystalline alloy surfaces would be an effective method to obtain an ideal material. The traditional heat treatment can achieve the whole crystallization, but it is difficult to reach the local crystallization [1,2]. So it is impossible to keep amorphous surface, while the other parts are crystallized by heat treatment. Laser [3–8] is a high energy density power, which has been used for material processing, such as laser welding, laser cladding, and laser heat treatment. Laser heat treatment is a kind of surface heat treatment technology, i.e., achieves surface heat treatment by heating metal material's surface using laser beam. Due to rapid heating and cooling which provides favorable conditions for the formation of amorphous phase, laser heat treatment is a useful method for the surface decrystallization of Zr-based crystalline alloys. The potential advantages of laser heat treatment also include small distortion, and high speed processing ability to treat the localized spot and approach inaccessible areas. Through laser heat treatment, microstructures, forming ability, and mechanical properties of the surface of alloys can be significantly improved [8]. Whereas only few works have focused on the theoretical basis. In this article, the hardness and free volume distributions of amorphous and crystalline samples treated by laser beam were studied to provide a theoretical basis for laser treating Zr-based crystalline alloy surfaces.

2. Experimental procedure

An ingot of $Zr_{41.2}Ti_{13.8}Ni_{10}Cu_{12.5}Be_{22.5}$ composition was prepared by arc melting the mixings of pure Zr, Ti, Ni, Cu, Be (99.99 mass%) metal under a Ti-gettered Ar atmosphere, and two metallic glass blocks(MGB) with 20 mm length, 20 mm width and 5 mm thickness were made by copper mold casting [9]. One MGB was made to crystallization by heat treatment at 730 K. Then, the two MGBs were treated in an Ar protection environment by laser beam with 2 mm diameter which is sent by the cross-flow continuous CO_2 laser with 10.6 um fixed wavelength. The microscopic structure was ascertained by micro-focused XRD with CuKa radiation, and mechanical properties were researched by nanoindentation experiment.

3. Calculation

Finite element method [10,11] was used to simulate the laser surface melting process with super high heating and cooling rates. This process was conducted to understand better the formation mechanism of the gradient structure of the laser-treated samples. A model of laser processing was first established using ANSYS. ANSYS is a kind of advanced Computer Aided Engineering tool. Corresponding to the real experiment conditions and process, the center of the upper surface of the specimen with 20 mm length, 20 mm width, and 5 mm thickness was loaded by heat flux at a power density of 255 W/mm^2 in the process of calculation. Heat flux was loaded into a 2 mm diameter circle region of the Gauss distribution. That is, the center power density was the largest, and the power density decreased with increasing radial distance. The bottom surface established an ideal contact with the half-infinite iron, whereas the other surfaces, except the loading region, dissipated heat by heat radiation. This model was last loaded by heat flux for 0.1 s and cooled for 5 s. Temperature distribution was then simulated. The temperature change obtained from the temperature field

* Corresponding author.
E-mail address: gongli@ysu.edu.cn (G. Li).

0022-3093/$ – see front matter
http://dx.doi.org/10.1016/j.jnoncrysol.2012.08.023

simulation was used as the boundary condition to enable stress change to be calculated.

4. Results

A laser beam-treated amorphous sample was polished carefully to smoothen the surface. The sample was then etched by an aqueous solution containing 50 ml HCl, 50 ml H_2SO_4, and 100 ml H_2O to observe the surface morphology under an optical microscope. Three distinct regions were observed [Fig. 1(a)]. As shown in Fig. 1(b), two distinct regions were observed in the crystalline sample under the same processing conditions.

In Fig. 1(a), the three regions along the radial direction of the spot treated by the laser beam are the amorphous center region (③), crystallizing orbicular region (②), and amorphous peripheral region (①). The two regions in Fig. 1(b) are the amorphous center region (④) and crystalline peripheral region (⑤). This conclusion was obtained through micro-focused XRD, as shown in Fig. 1(c). Regions ①, ③, and ④ are amorphous, whereas regions ② and ⑤ are crystalline. The corrosion phenomena of regions ①, ③, and ④ are relatively weak, whereas those of ② and ⑤ are stronger. This result verifies that the corrosion resistance of the amorphous phase is higher than that of the crystalline phase with the same composition.

The temperature change at every point in the model can be obtained through finite element simulation. Fig. 2(a) shows the time–temperature curves of the nine points distributed from the center to the radial direction of the spot. These points can achieve higher temperature with decreasing radial distance. Thus, in the amorphous sample, the points of the region with the highest temperature are larger than the solidification temperature T_m ($T>T_m$), which can be called the re-melting zone (i.e., region ③ in Fig. 1). $T_g<T<T_m$ can be called the heat-affected zone (i.e., region ② and the region of region ① near region ②). $T<T_g$ can be called the substrate region (i.e., region ① except the region near region ②). The heat-affected zone can be divided into two parts, namely, region ② ($T_x<T<T_m$) and the region of region ① near region ② ($T_g<T<T_x$). Based on the simulation results of the crystalline sample, $T>T_m$ can be called the re-melting zone (i.e., region ④), and $T<T_m$ can be called the crystalline region (i.e., region ⑤). The radial hardness variation of the two samples was measured through nanoindentation experiments,

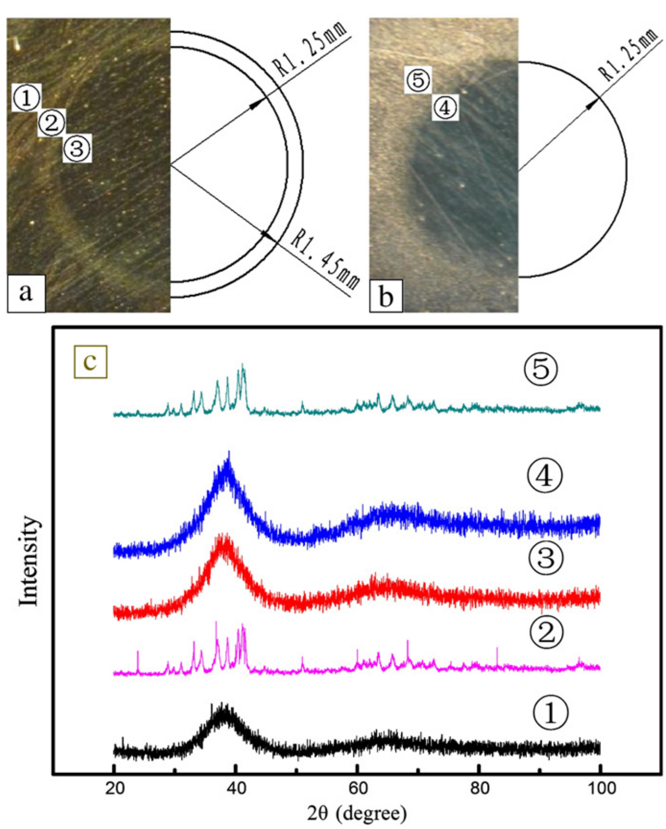

Fig. 1. (a) and (b) are optical micrographs with acid corrosion of amorphous and crystalline samples, respectively. (c) Micro-focused XRD results. The results indicate that ①, ③, and ④ are amorphous regions; ② and ⑤ are crystalline regions.

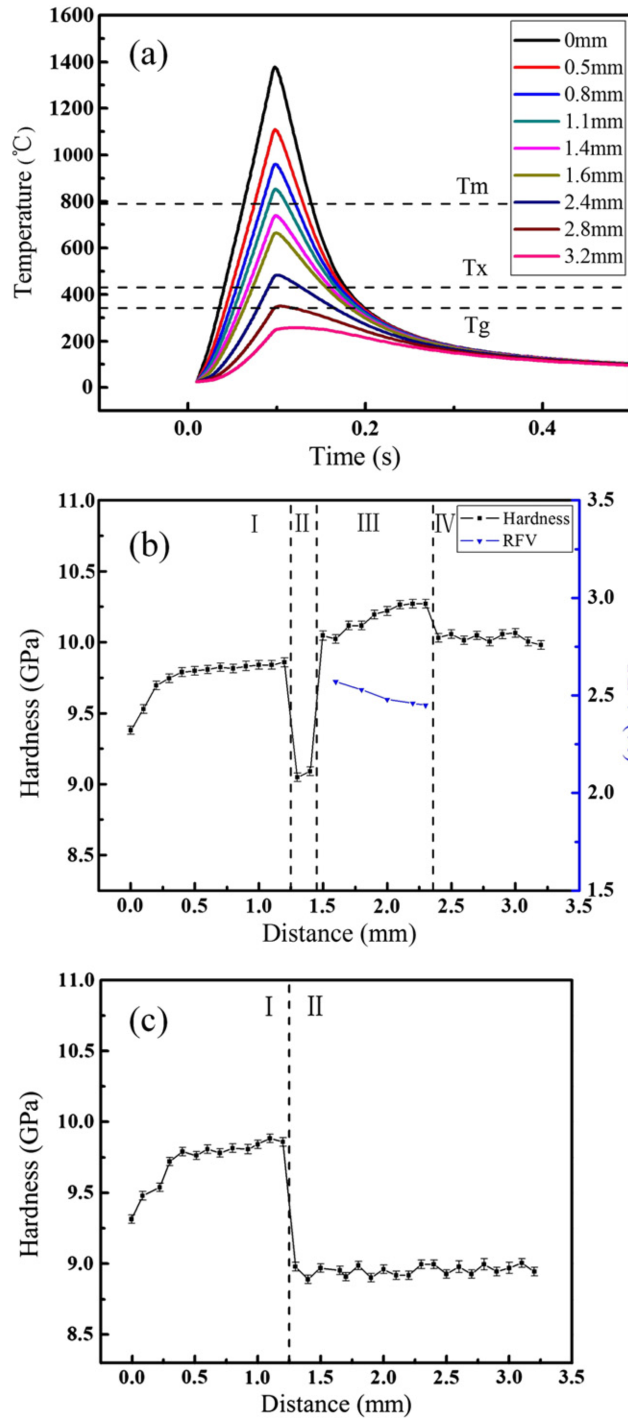

Fig. 2. (a) Time–temperature curves of the nine points distributed from the center of the spot along the radial direction. The distances indicate the radial distance of the corresponding points from the center of the spot. Three dash lines indicate the solidification temperature (T_m), crystallization temperature (T_x) and glass transition temperature (T_g), respectively. (b) and (c) are radial hardness distributions of amorphous and crystalline samples, respectively. The other curve in (b) shows the radial distribution of RFV. The dash lines are the boundaries of the different hardness regions.